A Role for Polo-like Kinase 4 in Mediation of Cytokinesis

Michael F. Press, Bin Xie, Simon Davenport, Yu Zhou, Roberta Guzman, Garry P. Nolan, Neil O'Brien, Michael Palazzolo, Tak W. Mak, Joan Brugge, and Dennis J. Slamon

Supporting Information Appendix.

Supporting Information, **SLegend Figure 4**.

Immunofluorescence localization of PLK4 to centrosomes, cleavage furrow and midbody is altered after CFI-400945 kinase inhibitor and/or MG115 protease inhibitor treatment. (**A**. Upper Left) Control HCT-116 colorectal carcinoma cells grown in either tissue culture medium alone (DMSO) or medium containing protease inhibitor MG115 (MG115). Immunofluorescence localization of PLK4 using commercially available anti-PLK4 antibody (P005, Cell Signaling antibody #3258) and gamma-tubulin in cells grown in culture medium with DMSO alone shows PLK4 localized weakly in centrosomes (arrow, left and right, {see C for higher magnification and better resolution of centrosomes}) and strongly in (much larger) midbodies (left and right). The inset includes an expanded image of the featured cell in order to better resolve the PLK4-labeled centrosome. The Cell Signaling antibody, #3258, recognizes an epitope that includes Cysteine-458 near the middle of the full-length protein. In contrast, treatment with MG115 protease inhibitor is associated with a dramatic increase in both the number of centrosomes that have co-localized PLK4 and the immunostaining intensity (presumed to be proportional to the amount) of PLK4 in each centrosome (MG115 compared to DMSO). Strikingly, the midbodies that were prominently identified in the absence of MG115 (see A {DMSO, right panel} and C) are inconspicuous with MG115 protease inhibitor treatment (see A MG115, right panel). (**B**. Middle Left) Immunofluorescence localization of PLK4 with the same anti-PLK4 antibody (P005, Cell Signaling #3258) after treatment with the PLK4 kinase inhibitor CFI-400945 (CFI-945) is associated with localization only to centrosomes (gamma-tubulin positive {green}, left, and PLK4 alone on right {red}). Note the absence of PLK4 immunostaining in any structures other than gamma-tubulin-positive centrosomes and the slightly greater intensity of the red centrosome signals compared to A. Compared to A/DMSO, A/MG115 and B/CFI-945 show a striking loss of red IF immunostaining in midbodies. Finally, immunofluorescence co-localization of PLK4 (red) with gamma-tubulin (green) when treated with both CFI-400945 PLK4 kinase inhibitor and MG115 protease inhibitor (CFI-945/MG115) demonstrate strong localization of PLK4 almost exclusively to centrosomes. Few, if any, midbodies are present with PLK4 (red) localization. The centrosomes are more brightly IF stained red compared to any of the previous conditions. (**C**. Upper Right) Due to the low magnification, panel A does not facilitate demonstration of endogenous PLK4 localization in centrosomes with sufficient resolution. Therefore, higher magnification photomicrographs are used here for this purpose. PLK4 is identified in centrosomes, for example the boxed area contains two centrosomes and a midbody that are shown at higher magnification both with gamma-tubulin (green) localization (left) and without gamma-tubulin but with PLK4 localization (arrows, red IF) corresponding to the site of the two (small) centrosomes. The much larger midbody (center right) shows localization of PLK4 as well. (**D**. Lower Left) Phospho-serine305-PLK4 (red)(Ab#3) localization to the midbodies and cleavage furrow as confirmed by co-localization of phospho-PLK4 and MKLP1 (mitotic kinesin-like protein-1, a midbody protein involved in cellular abscission) to the same subcellular structures, i.e. cleavage furrow and midbody (arrows). Photomicrographs A, B, C and D at original magnifications of 200x. Insert of figure C 700x. **E**. (Lower Right) The average numeric distribution of PLK4 in centrosomes and midbodies per 500 tumor cells demonstrates the substantial loss of PLK4-positive midbodies with either CFI-900945 or MG115 or treatment with both and the substantial increase in the number of PLK4-positive centrosomes. See also SI Appendix, Movies S1-S6 for time-lapse video-microscopy that demonstrates the inability of CFI-400945 PLK4 inhibitor-treated OVCAR3, HCT-116 and CAL51 human ovarian cancer, human colorectal cancer and human breast cancer cells to complete cytokinesis compared to control DMSO-treated cells that can complete cytokinesis.

Figure S1. Expression of PLK4 (P005) and phospho-PLK4 (Ab3) in colorectal and breast cancer cell lines, related to Figure 3.

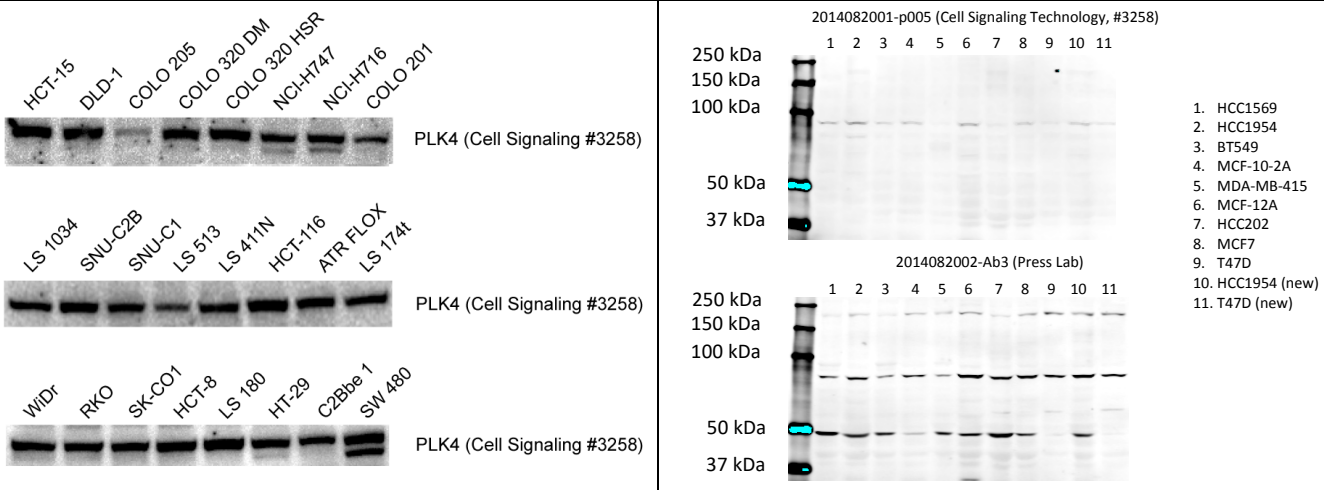

Figure S1. Western immunoblot analyses of 24 different colorectal cancer, 7 different breast cancer, and 2 non-malignant breast epithelial cell lines to demonstrate full-length PLK4 (left and upper right) and phospho-PLK4 (right lower blot), related to Figure 3. The left and right upper western blots demonstrate full-length (97 kDa) PLK4 with a commercially available anti-PLK4 antibody (P005, Cell Signaling #3258). The right, lower western blot was performed using the same filter as the above western blot, but after extensive washing with buffer and re-probing with an anti-phospho-PLK4 antibody (Ab3). Please note that the phospho-PLK4 in the lower filter is of smaller size, approximately 75 and 50 kDa. Cultured cells were not synchronized with regard to cell cycle. We confirmed that the smaller bands corresponded to pPLK4 by using immunoprecipitation assays followed by mass spectrometry to assess the amino acid sequence of precipitated proteins (sequencing data described in Results).

Figure S2. Specificity of anti-phospho-PLK4 antibody for PLK4 confirmed by PLK4-specific small inhibitory RNA in breast and ovarian cancer cell lines, related to Figures 2, 4 and 6.

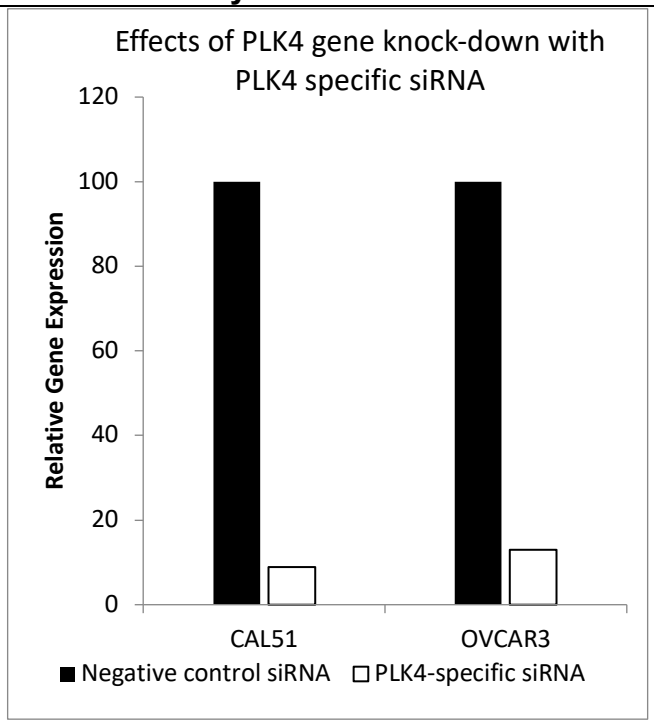

A. PLK4 messenger RNA expression by quantitative PCR using control scrambled compared to PLK4-specific siRNA transfected breast and ovarian cancer cell lines.

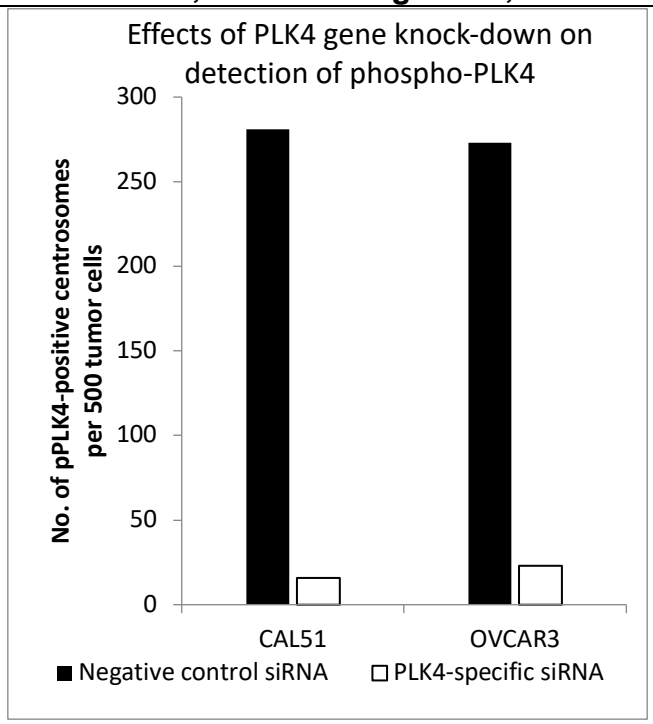

B. Expression of phospho-PLK4 protein in human breast and ovarian cancer cell lines transiently transfected with control and PLK4-specific small inhibitory RNA.

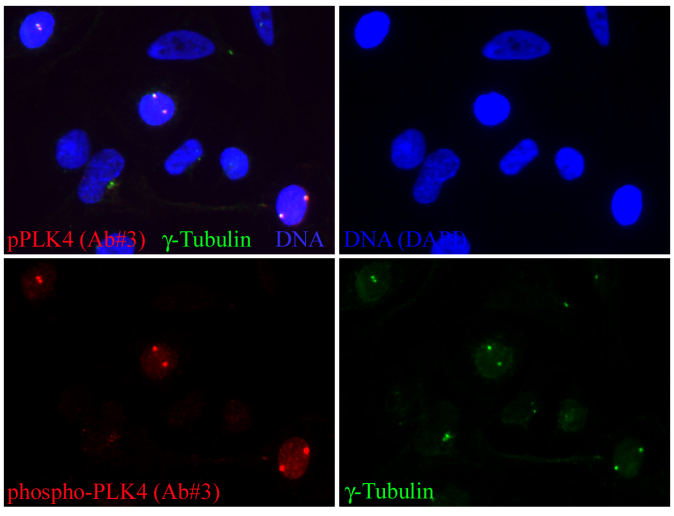

C. Human breast cancer cells transiently transfected for 96 hours with negative control (scrambled) siRNA showing immunofluorescence (IF) localization of phospho-PLK4 to centrosomes using our anti-phospho-PLK4 antibody, Ab#3.

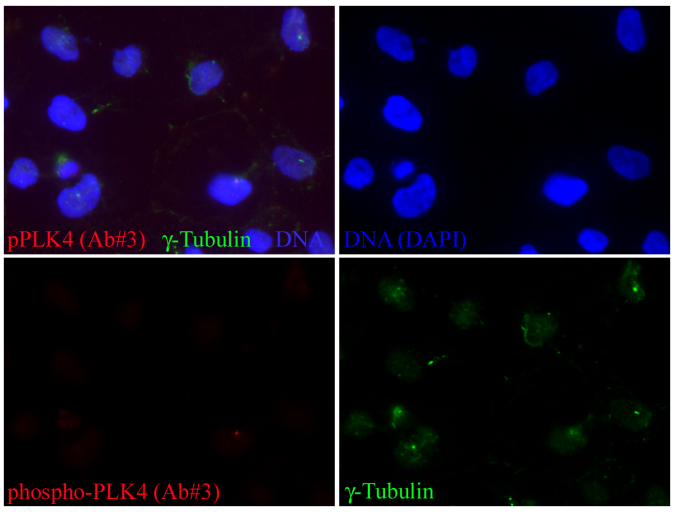

D. Human breast cancer cells transiently transfected with PLK4-specific small inhibitory RNA showing a relative LACK of IF localization of phospho-PLK4 to centrosomes (only one phospho-PLK4-positive centrosome) using our anti-phospho-PLK4 antibody, Ab#3.

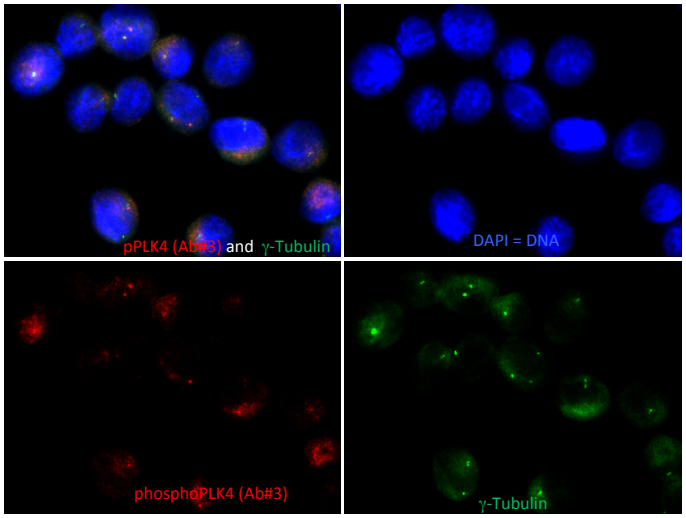

E. Human OVCAR3 ovarian cancer cells transiently transfected with negative control (scrambled) siRNA showing immunofluorescence (IF) localization of phospho-PLK4 to centrosomes using our anti-phospho-PLK4 antibody, Ab#3.

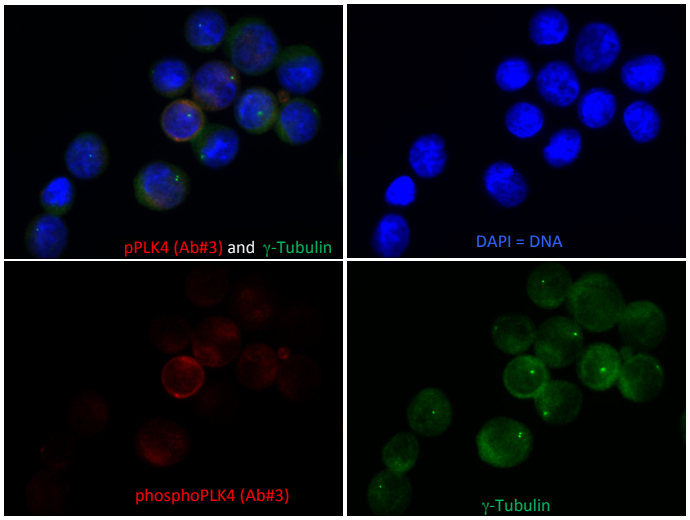

F. Human OVCAR3 ovarian cancer cells transiently transfected with PLK4-specific small inhibitory RNA show a LACK of IF localization for phospho-PLK4 to centrosomes using our anti-phospho-PLK4 antibody, Ab#3.

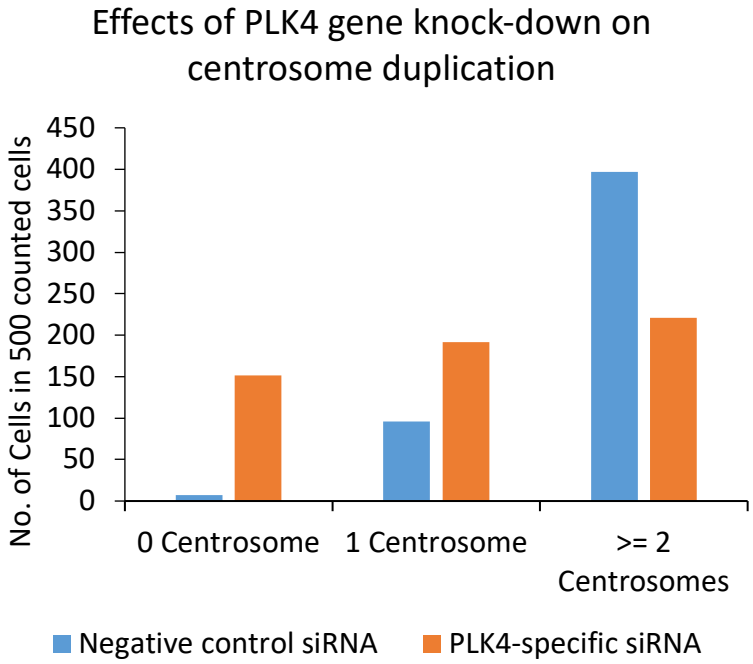

G. Functional effect of treatment with PLK4-specific small inhibitory RNA on centrosome duplication over 96 hours. The number of centrosomes identified with anti-gamma tubulin antibody by IF in OVCAR3 human ovarian cancer cells transiently transfected with PLK4-specific small inhibitory RNA is significantly reduced compared to control treated cells over a 96-hour period. Approximately 80% of control-treated cells contain two centrosomes, 19% of control-treated cells have one centrosome, and only 1% have no centrosomes. In contrast, the distribution of centrosomes in cells treated with PLK4-specific siRNA is different. Many (27%) have no centrosomes, a third (34%) have one centrosome and only slightly more than a third (39%) have two centrosomes. This indicates that inhibition of PLK4 expression interferes with centromere duplication, as expected.

Figure S3. siRNA knock-down of *PLK4* gene expression in HCT-116 colorectal cancer cells is associated with lack of centrosome duplication, related to Figure 4.

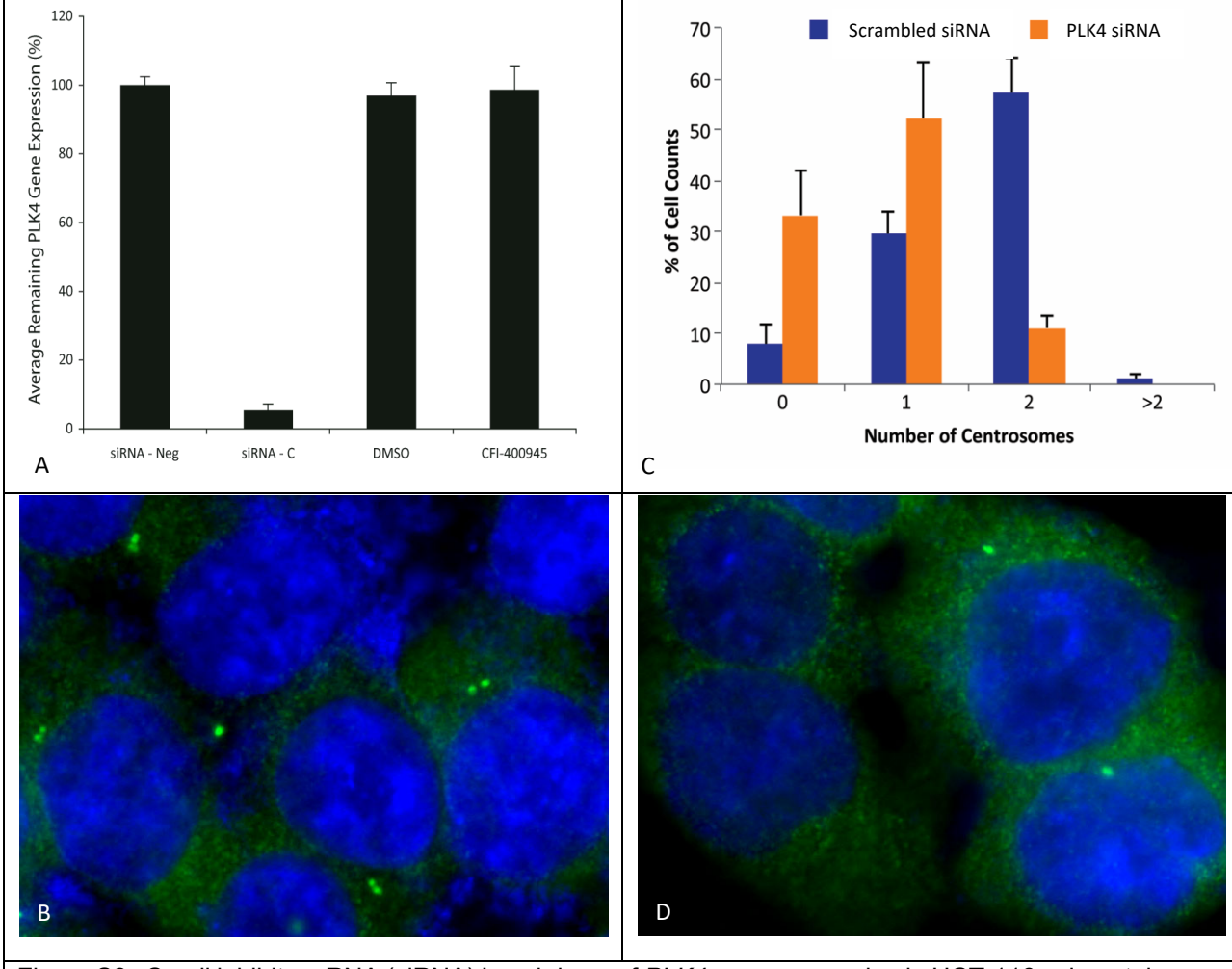

Figure S3. Small inhibitory RNA (siRNA) knockdown of *PLK4* gene expression in HCT-116 colorectal cancer cells is associated with lack of centrosome duplication. A, upper left panel. Assessment of *PLK4* gene expression using reverse transcriptase-polymerase chain reaction after 24 hours incubation with, from left to right, scrambled control siRNA (siRNA-Neg), *PLK4* siRNA (siRNA-C), diluent (DMSO) added, and addition of PLK4 inhibitor CFI-400945. Only the addition of *PLK4* siRNA to the culture medium reduced mRNA expression (>90%) of *PLK4*. B, lower left. Immunofluorescence localization of centrosomes using an anti-gamma-tubulin antibody confirms centrosome duplication in HCT-116 colorectal cancer cell lines in medium containing a control scrambled siRNA. D, lower right. Localization of centrosomes by immunofluorescence with anti-gamma-tubulin antibody demonstrates that the majority of HCT-116 colorectal cancer cells treated for 48 hours with *PLK4* siRNA contain only a single centrosome. C, upper right. Bar graph plot of number of centrosomes identified in unsynchronized HCT-116 colorectal cancer cells after 48 hours of treatment with either control scrambled siRNA (blue) or *PLK4* siRNA (orange). While the majority (>50%) of HCT-116 cells in control siRNA-containing medium had duplicated the centrosome, only a small minority (<10%) of HCT-116 cells contained two centrosomes. The majority of *PLK4*-siRNA-treated cells failed to duplicate the centrosome and had one centrosome per cell and some (<10%) lacked any identifiable centrosome, presumably because the cells failed to duplicate their centrosome but had completed cytokinesis.

Figure S4. Transient transfection with *PLK4*-mutant (kinase-inactive or "kinase dead") (KD) and *PLK4*-wildtype (WT) in an enhanced green fluorescence protein expression vector (pEGFP-C1), related to Figure 4.

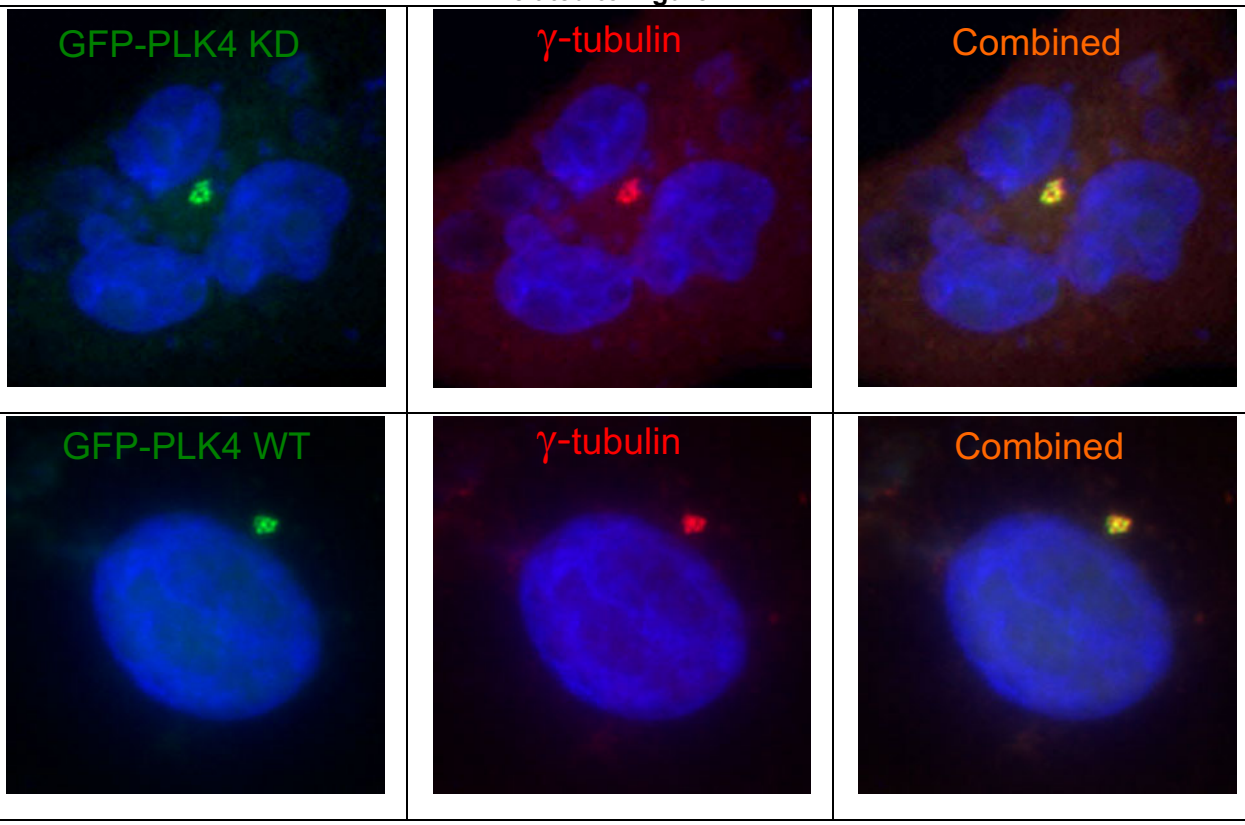

Figure S4. Transient transfection with *PLK4*-mutant (kinase-inactive or "kinase dead") (above) and *PLK4*-wildtype (below) in the enhanced green fluorescence protein expression vector (pEGFP-C1), related to Figure 4. Both transfectants showed centrosome amplification; however, only GFP-*PLK4*-KD transfectants were associated with multi-lobed nuclei or multiple nuclei in a substantial percentage of the cells.

Figure S5. Treatment of HCT-116 colorectal cancer cells with PLK4 inhibitor CFI-400945 for 24 hours, related to Figures 4 and 5.

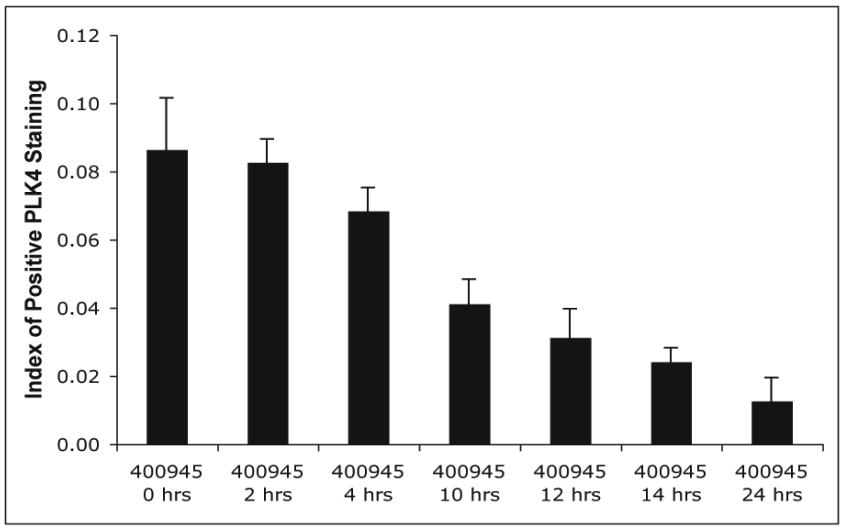

A.

Treatment of colorectal cancer cell lines for 24 hours is associated with a reduced number of cells containing PLK4-positive midbodies (A), as well as with increased nuclear size and nuclear complexity in both xenografts (B), and cultured cells (C, D).

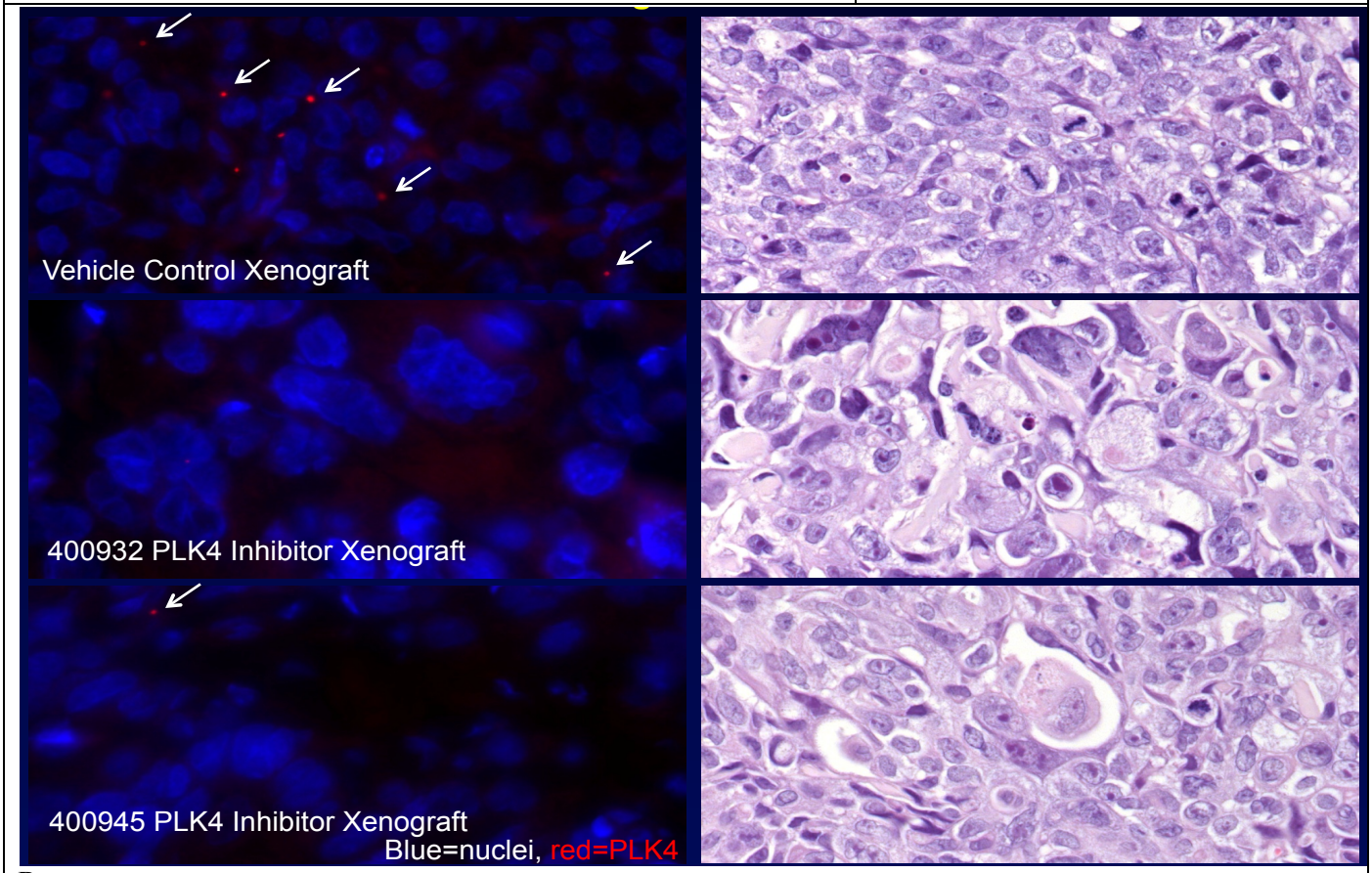

B.

B. Reduction in PLK4-positive midbodies in HCT-116-containing xenografts. Top panels, left and right. Immunofluorescence localization of PLK4 to midbodies (top left, red=PLK4) in HCT-116 xenografts after treatment for 24 hours with vehicle control. In the top right photomicrograph of a hematoxylin-and-eosin stain tissue section, please note the relative uniformity of nuclear size with abundant mitotic figures among the tumor cells. Middle and

Bottom, left and right. HCT-116 xenografts treated once at time zero with two different PLK4 inhibitors (CFI-400932 {208 mg/kg}, middle panels and CFI-400945 {130 mg/kg} lower panels). Left, middle and bottom panels show relative lack of PLK4-positive midbodies. Considerable effort was required to locate even the single PLK4-positive midbody illustrated in these two panels. Right, middle and bottom panels demonstrate lack of mitotic figures, increased nuclear size and complexity with multi-lobed or multiple nuclei per tumor cell in many cells.

PLK4 α-Tubulin DAPI

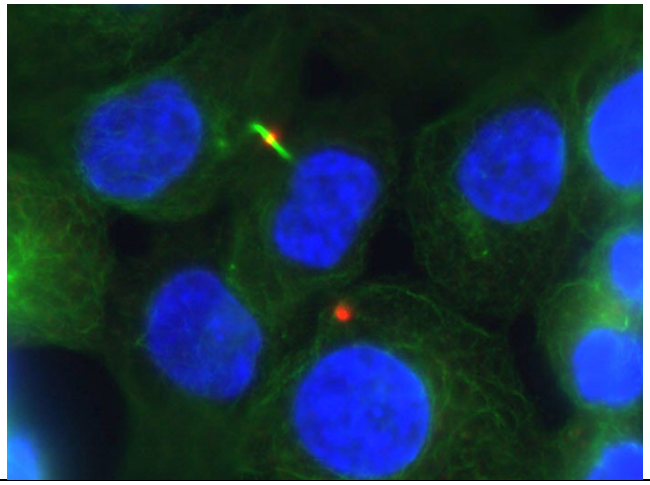

C. HCT-116 colorectal cancer cells after control (DMSO) treatment for 24 hours. PLK4 and alpha-tubulin are localized by immunofluorescence.

PLK4 α-Tubulin DAPI

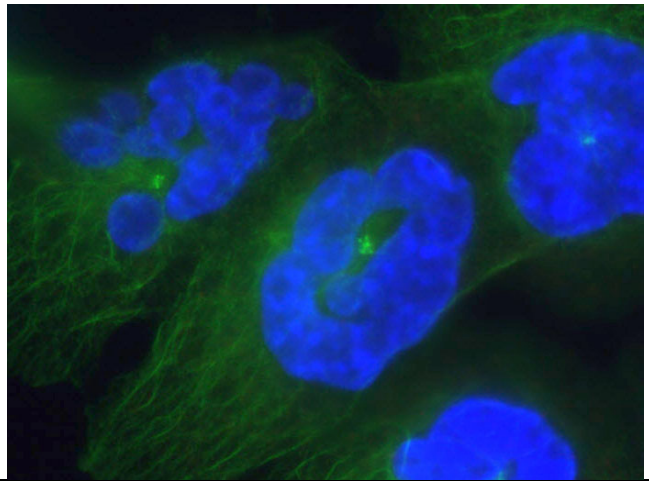

D. HCT-116 colorectal cancer cells after CFI-400945 PLK4 inhibitor treatment for 24 hours (50 nM) is associated with a substantial reduction (near absence) in the number of cells with PLK4 localization in midbodies, and an increased frequency of centrosome amplification and polyploid, multi-lobed nuclei.

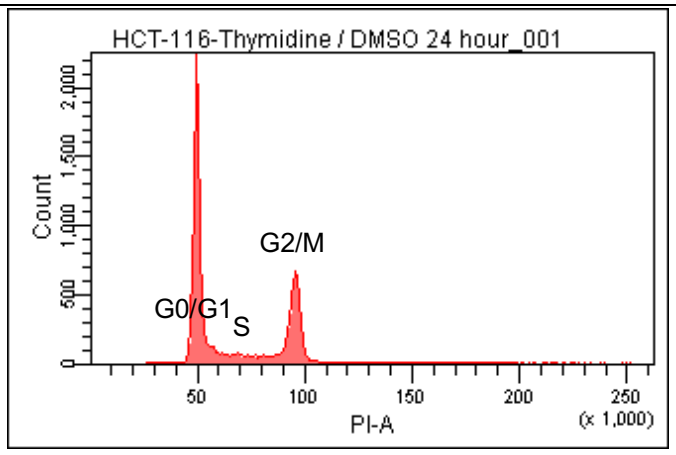

E. Flow cytometry of control HCT-116 cells. The modal DNA peak (G0/G1) indicates the baseline content of DNA followed by increased DNA content during S-phase and, finally, double the DNA content in G2/M phase cells.

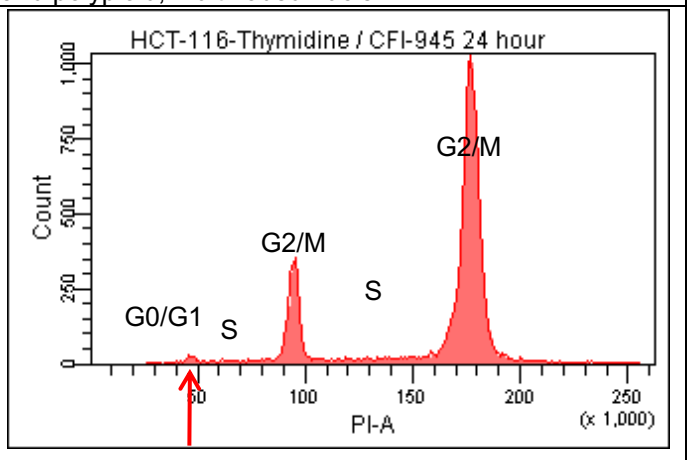

F. Flow cytometry of CFI-400945 treated HCT-116 cells. The location of the original (and control) modal DNA peak is indicated (red arrow, G0/G1). Over 24 hours there is no return to the modal DNA content since tumor cells accumulate additional DNA with each S-phase; however, they clearly do not complete cytokinesis.

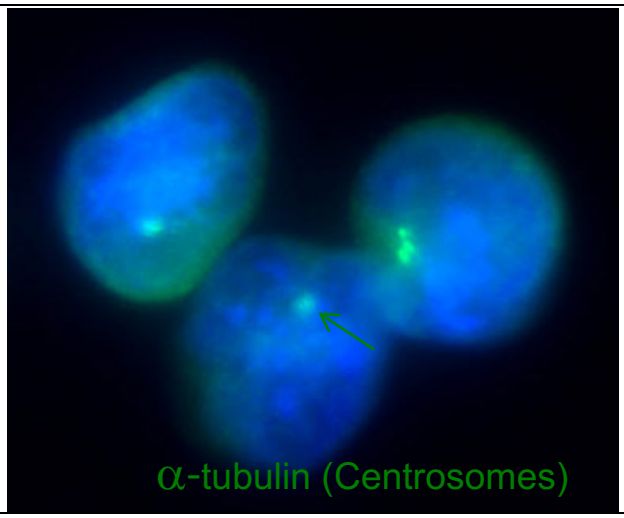	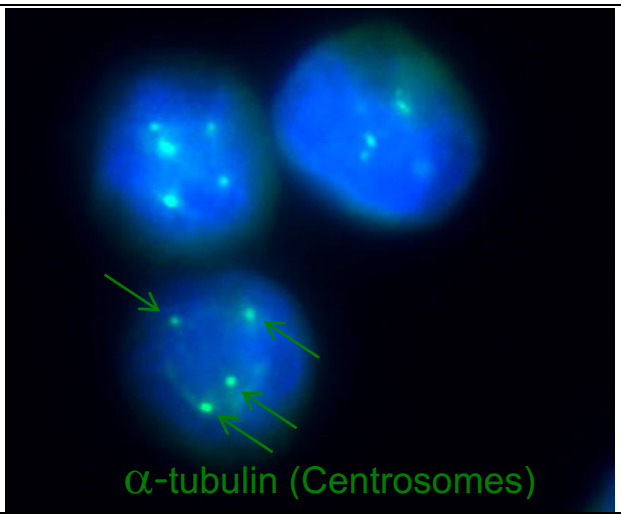
G. Immunofluorescence localization of alpha-tubulin to identify centrosomes in control (DMSO) treated HCT-116 cells.	H. Immunofluorescence localization of alpha-tubulin to identify centrosomes in CFI-400945 PLK4 inhibitor-treated HCT-116 cells.

SI Appendix: Movies. Time-lapse videomicroscopy of control (DMSO) and CFI-400945 PLK4 inhibitor-treated OVCAR3, HCT-116 and CAL51 cell lines, related to Figures 4 and 6.	
	
Movie S1. Control OVCAR3 human ovarian carcinoma cells. Time-lapse videomicroscopy of synchronized, control (DMSO treated) ovarian cancer cells demonstrates orderly progression through M-phase with separation of daughter cells to approximately double the number of cells present in this field at the conclusion of 18 hours of observation. In the entire microscopic field from which this video was cropped (due restrictions on size), at time 0, n = 165 cells; and at time 18 hours, n = 237 cells). Doubling time for OVCAR3 cells is approximately 24 hours. **REFER TO VIDEOMICROSCOPY SUPPLEMENTAL Movie S1.**	Movie S2. CFI-400945 PLK4 inhibitor-treated OVCAR3 human ovarian carcinoma cells. Time-lapse videomicroscopy of synchronized ovarian cancer cells treated for 18 hours with PLK4 inhibitor (50 nM) demonstrate an inability to complete cytokinesis. The cells rapidly round up, the nuclear envelope disappears, and chromosomes condense; however, the nuclei enlarge but remain coalesced as a single large nucleus and the cells fail to separate into daughter cells. In the entire microscopic field from which this video was cropped (due restrictions on size), at time 0, n = 138 cells; and at time 18 hours, n = 138 cells). **REFER TO VIDEOMICROSCOPY SUPPLEMENTAL Movie S2.**
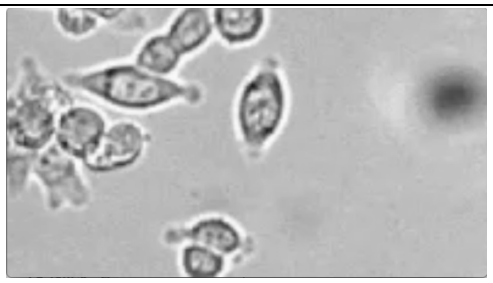	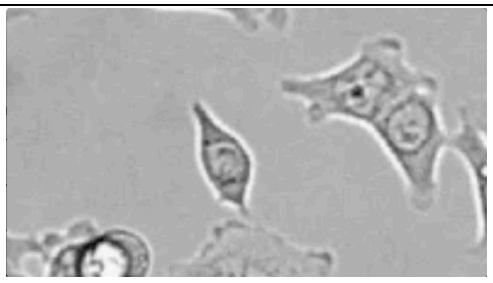
Movie S3. Control HCT-116 human colorectal carcinoma cells. Time-lapse videomicroscopy of synchronized, control (DMSO treated) colorectal cancer cells demonstrates orderly progression through M-phase with separation of daughter cells to approximately double the number of cells present in this field at the conclusion of 18 hours of observation. In the entire microscopic field from which this video was cropped (due restrictions on size), at time 0, n = 150 cells; at time 18 hours, n = 313 cells). Doubling time of HCT-116 cells is approximately 24 hours. **REFER TO VIDEOMICROSCOPY SUPPLEMENTAL Movie S3.**	Movie S4. CFI-400945 PLK4 inhibitor-treated HCT-116 human colorectal carcinoma cells. Time-lapse videomicroscopy of synchronized, HCT-116 cells treated with PLK4 inhibitor (50 nM) for approximately 18 hours demonstrates that the cells round up to enter M-phase, condense chromosomes in the metaphase plate and form two separate nuclei; however, the cells do not separate into daughter cells and, therefore, create large cells with polyploid nuclei. Although the number of nuclear profiles is increased, the number of cells is not increased. In the entire microscopic field from which this video was cropped (due restrictions on size), at time 0, n = 116 cells; while at time 18 hours, n = 105 cells). **REFER TO VIDEOMICROSCOPY SUPPLEMENTAL Movie S4.**

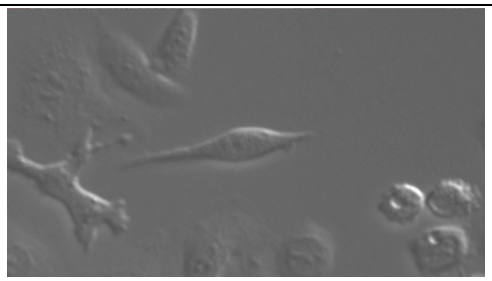	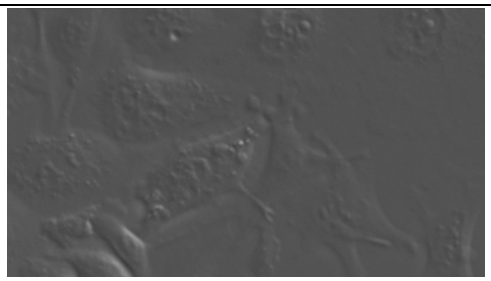
Movie S5. Control CAL51 human breast carcinoma cells. Time-lapse videomicroscopy of synchronized, control (DMSO treated) breast cancer cells demonstrates orderly progression through M-phase with separation of daughter cells to approximately double the number of cells present in this field at the conclusion of 22 hours of observation. In the entire microscopic field from which this video was cropped (due restrictions on size), at time 0, n = 97 cells; and at time 22 hours, n = 233 cells). Doubling time for CAL51 cells is approximately 24 hours. **REFER TO VIDEOMICROSCOPY SUPPLEMENTAL Movie S5.**	Movie S6. CFI-400945 PLK4 inhibitor-treated CAL51 human breast carcinoma cells. Time-lapse videomicroscopy of synchronized breast cancer cells treated for 22 hours with PLK4 inhibitor (50 nM) demonstrate an inability to complete cytokinesis. The cells rapidly round up, the nuclear envelope disappears, and chromosomes condense; however, the nuclei enlarge but remain coalesced as a single large nucleus and the cells fail to separate into daughter cells. In the entire microscopic field from which this video was cropped (due restrictions on size), at time 0, n = 80 cells; and at time 22 hours, n = 79 cells). **REFER TO VIDEOMICROSCOPY SUPPLEMENTAL Movie S6.**
We suggest reducing the movie viewing window to the minimum size in order to maintain resolution.	